Available online at www.sciencedirect.com
SCIENCE DIRECT®
ELSEVIER
Archives of Biochemistry and Biophysics 428 (2004) 52–63
ABB
www.elsevier.com/locate/yabbi

Minireview

Molecular engineering of PQQGDH and its applications

Satoshi Igarashi,[a,*] Junko Okuda,[a] Kazunori Ikebukuro,[b] and Koji Sode[b,*]

[a] *National Institute for Materials Science, 1-1, Namiki, Tsukuba, Ibaraki, 305-0044, Japan*
[b] *Department of Biotechnology, Tokyo University of Agriculture and Technology, 2-24-16, Naka-cho, Koganei, Tokyo, 184-8588, Japan*

Received 4 March 2004, and in revised form 7 June 2004

Two types of glucose dehydrogenases harboring PQQ as their prosthetic group have been reported [1,2]. The first type is the membrane-bound glucose dehydrogenase (PQQGDH-A), which has been isolated from various Gram-negative bacteria including *Escherichia coli*, *Acinetobacter calcoaceticus*, *Pseudomonas* sp., and acetic acid bacteria [3]. PQQGDH-As are all single peptides of approximately 87-kDa MW, containing one PQQ molecule [4,5]. The physiological role of PQQGDH-A in bacteria is the terminal oxidation of glucose coupled with the respiratory chain via ubiquinone [6,7]. The 3-D structure of PQQGDH-A is predicted to be a β-propeller fold composed of eight W motifs, based on analogy with PQQ-harboring methanol dehydrogenase [8] and the result of CD spectroscopy of the enzyme in which the N-terminal membrane-spanning region had been deleted [9]. The N-terminal region is predicted to be a membrane-spanning anchor region [10]. Our groups have reported several site-directed mutagenesis studies on PQQGDH-A including the first report [11–21].

The second type of glucose dehydrogenase harboring PQQ is the water-soluble PQQGDH-B isolated from the genus *A. calcoaceticus*. PQQGDH-B does not share any obvious primary structure homology with other PQQ enzymes [22]. PQQGDH-B is a homodimeric, with each 50-kDa monomer containing one PQQ molecule and three Ca^{2+} ions, two of which are located in the dimer interface and the third ion is bound near the PQQ [22–24]. PQQGDH-B is not coupled to the respiration chain of *A. calcoaceticus* and its physiological role remains to be elucidated. This enzyme catalyzes the oxidation of glucose, allose, 3-*O*-methyl-glucose as well as the disaccharides lactose, cellobiose, and maltose [25]. PQQGDH-B has a broader substrate specificity profile than PQQGDH-A. PQQGDH-B contains an N-terminal 24-amino acid signal peptide, which is excised after secretion to the periplasm. Although it has a β-propeller structure similar to other quinoproteins, the PQQGDH-B β-propeller fold is composed of only six W motifs [24]. PQQ resides in a deep, broad, positively charged cleft at the top of the propeller near the 6-fold pseudo-symmetry axis [26]. The active site of PQQGDH-B is composed of loops 1D2A, 2D3A, 3BC, 4D5A, and 6BC (see Table 5 and Fig. 4). The reported substrate binding residues are located mainly on loops 1D2A, 2D3A, and 3BC [26].

PQQGDHs are the most industrially attractive among the several PQQ-harboring enzymes. PQQGDHs has now become the major enzyme used in sensor systems for self-monitoring of blood glucose (SMBG).[1] Glucose oxidase (GOD) has been utilized as the most reliable and economic enzyme for glucose monitoring since the early biosensor development. However, GODs inherent requirement for oxygen as the electron acceptor limits its further application in the artificial electron mediator-based electrochemical enzyme sensor [27–29]. Focusing on PQQGDHs' independence on oxygen as electron acceptor, various glucose sensors employing PQQGDHs have been reported [30–38].

The merits of using PQQGDHs for glucose sensors include the following: (i) PQQGDHs show higher catalytic efficiency than GOD, thus enabling rapid glucose sensing. (ii) Because PQQ is tightly bound to GDH, the

* Corresponding authors.
E-mail addresses: igarashi.satoshi@nims.go.jp (S. Igarashi), okuda.junko@nims.go.jp (J. Okuda), ikebu@cc.tuat.ac.jp (K. Ikebukuro), sode@cc.tuat.ac.jp (K. Sode).

[1] *Abbreviations used:* SMBG, self-monitoring of blood glucose; GOD, glucose oxidase; CGM, continuous glucose monitoring; FIA, flow injection analysis; PMS, phenazine methosulfate; mPMS, 1-methoxy-5-methylphenazinium methylsulfate; QH-EDH, quinohemoprotein ethanol dehydrogenase; BOD, bilirubin oxidase; SNP, single nucleotide polymorphisms.

0003-9861/$ - see front matter © 2004 Elsevier Inc. All rights reserved.
doi:10.1016/j.abb.2004.06.001

addition of extra co-factors, such as NAD(P), is not necessary. (iii) PQQGDHs do not utilize dissolve oxygen as electron acceptor during glucose oxidation, thus contributing to the accuracy of measurement of glucose in human blood.

Principally because of these merits, PQQGDH-B-employing glucose sensors have already found their way onto the market. However, despite these superior features, further improvements of PQQGDHs enzymatic properties are required together with the recombinant production of PQQGDHs. This is particularly true when PQQGDHs are compared with GOD, which has better substrate specificity and operational stability.

The authors' research group is the pioneer and the only group to have engaged in the protein engineering of PQQGDHs, which we have done to develop an ideal glucose sensor enzyme [25,39–43]. We also developed several novel methods for the efficient production of recombinant PQQGDH-B, including the use of *Klebsiella* and metabolically engineered *E. coli* as host microorganisms [44], secretional production in yeast [45], and engineering the surface charge the enzyme to facilitate its preparation [46]. This review summarizes our current status of PQQGDH-B molecular engineering and their applications.

PQQGDH-B engineering by site-directed mutagenesis studies

Prior to the elucidation of the tertiary and quaternary structures of this enzyme, we had been carrying out protein engineering of PQQGDH-B to improve its enzymatic properties, such as substrate specificity and stability. The various engineering approaches we followed also provided several basic information essential to understanding the enzyme mechanism of PQQGDH-B, which are summarized in this section.

Catalytic center

Since Oubrie et al. [24,26] elucidated the 3-D structure of PQQGDH-B, the amino acid residues making up the active site have also been proposed. Although His168 had been proposed to have a crucial role in the oxidation of glucose, no experimental evidence was available to support this. We constructed two His168 mutants of PQQGDH-B, His168Cys and His168Gln, that showed drastically reduced k_{cat} values (2.5 and 0.8 s^{-1}, respectively) and increased K_m values (193 mM and 154 mM, respectively). The catalytic efficiencies (k_{cat}/K_m) of His168Cys ($12.9 \times 10^{-3}\ s^{-1}\ mM^{-1}$) and His168Gln ($5.2 \times 10^{-3}\ s^{-1}\ mM^{-1}$) are 11,900- and 29,600-fold lower than that of the wild-type enzyme ($154\ s^{-1}\ mM^{-1}$). Based on the 3-D structure of PQQGDH-B [26], His168 was proposed to be positioned in the active center and function as a base catalyst in direct hydride transfer. The greatly decreased catalytic efficiencies resulting from mutation of His168 are consistent with this residue playing a significant role in the oxidation of substrates.

In addition to His168, several residues that may be involved in the catalytic reaction and/or substrate binding have been found to be essential for the expression of GDH activity. In the PQQGDH-B–glucose complex structure (PDB code: 1CQ1), hydrogen bonds have been identified between the glucose O1 atom and Arg252 as well as between the glucose O2 atom and Gln100. Substitution of Gln100 with Ala, Glu, Phe, Gly, Lys, Leu, Asn, or Ser as well as substitution of Arg252 with Ala, Glu, Gly, His, Lys, or Gln both resulted in almost complete abolishment of activity. These results are consistent with the essential role of the two residues at the catalytic center. The residues directly interact with substrate are essential for enzyme activity, but both PQQ binding site and Ca^{2+} binding site are also inevitable for enzyme activity. We have obtained the results of the decrease in enzyme activity by the introduction the mutations into these sites.

Substrate specificity

Improvement of the substrate specificity profile of PQQGDH-B is one of our ultimate goals of our protein engineering. Prior to the elucidation of the 3-D structure of PQQGDH-B, we initiated site-directed mutagenesis studies on PQQGDH-B based on the enzymatic properties of random mutant generated by error-prone PCR [25]. We found that the substitution of Glu277 residue resulted in a drastic decrease in EDTA tolerance, which is used as an indicator of bivalent metal binding stability. Among the Glu277 variants we generated, Glu277-Lys showed similar enzymatic activity and thermal stability to the wild-type enzyme, but its catalytic efficiency ($349\ s^{-1}\ mM^{-1}$) was approximately twice that of the wild-type enzyme ($154\ s^{-1}\ mM^{-1}$) (Table 1). This mutant enzyme showed narrower substrate specificity than that of the wild-type enzyme (for maltose; 48–20%, maltotriose; 69–28%).

According to the 3-D structure of PQQGDH-B, Glu277 is located on strand 4C, which is connected to loop4BC, one of the loop regions that create the enzyme's cavity. Glu277 mainly interacts with Ca^{2+} ion (II) that is located at the dimer interface loop region. Therefore, the replacement of Glu277 with other amino acids may affect its dimer conformation. Furthermore, the neighboring amino acid residue, Asp275, apparently works as one of the residues connecting a water molecule to Ca^{2+} ion (III). Asp276 is part of the Ca^{2+} ion-binding site (I) that is located at an active site. In addition, Asn279 also contributes in connecting a water molecule to Ca^{2+} ion (III). Thus the region from Asp275 to Asn279 is a critical region related to all Ca^{2+}

Table 1
Kinetic Parameters of PQQGDH-B Wild-Type and Glu277Lys

	Wild-type			Glu277Lys		
	K_m (mM)	k_{cat} (s^{-1})	k_{cat}/K_m (s^{-1} mM^{-1})	K_m (mM)	k_{cat} (s^{-1})	k_{cat}/K_m (s^{-1} mM^{-1})
Glucose	25.0	3860	154(100%)	8.8	3071	349(100%)
Allose	35.5	2509	71(46%)	21.0	4563	217(62%)
3-*O*-methyl-glucose	28.7	3011	105(68%)	27.0	3198	118(34%)
Galactose	5.3	232	44(29%)	6.8	630	92(26%)
Lactose	18.9	1659	88(57%)	7.5	1795	239(68%)
Maltose	26.0	1930	74(48%)	14.3	1015	71(20%)
Cellobiose	14.0	1355	97(63%)	8.5	1668	196(56%)
Maltotriose	13.9	1230	88(69%)	7.0	671	96(28%)

ion-binding sites and the active site of PQQGDH-B. We can conclude that the decreased EDTA tolerance and thermal stability are consistent with the location and function of these residues.

In the C-terminal region of PQQGDH-A, the conserved amino acid residues His775 (in *E. coli* PQQGDH) and His781 (in *A. calcoaceticus* PQQGDH-A) were shown to be responsible for their substrate specificity profiles [14,17]. Although the primary structure of PQQGDH-B has little similarity to that of PQQGDH-As, the active site orientation in both enzymes is opposite to where the C- and N-termini close the circular β-propeller structure. Based on this similarity, we assumed that residues with the same 3-D orientation would have the same affect on substrate specificity of both PQQGDH-A and PQQGDH-B, thus making the C-terminus the region of interest. Moreover, according to structural information of the PQQGDH-B active site, the glucose substrate is located in a cavity composed of loops 1D2A, 2D3A, 3BC, 4D5A, and 6BC, and interacts with amino acid residues located on loops 1D2A, 2D3A, and 3BC [26]. However, loop 6BC does not have amino acid residues that interact directly with glucose. Viewing the active site structure, the putative interacting site to the non-reducing group of disaccharides is corresponded to the C-terminus of PQQGDH-B especially loop 6BC. Therefore, we introduced amino acid substitutions into this region to improve the substrate specificity profile. We constructed a series of mutants focusing on polar amino acid residues within the loop 6BC region. Among these mutants, we found that Asn452Thr showed a narrowed substrate specificity profile without a decrease in catalytic activity (Table 2) [41].

Based on the results from the His168 mutants, substitutions were carried out on the neighboring residues Lys166, Asp167, and Gln169, in an attempt to alter the enzyme's substrate binding site. Lys166 and Gln169 mutants showed only minor changes in substrate specificity profiles. In sharp contrast, mutants of Asp167 showed considerably altered specificity profiles [43]. Of the numerous Asp167 mutants characterized, Asp167Glu showed the best substrate specificity profile, while retaining most of its catalytic activity for glucose and high stability. The activities of Asp167Glu for the disaccharides lactose and maltose, relative to glucose, were decreased to 19 and 10%, respectively, compared to the wild-type relative activities of 57 and 48%, respectively (Table 3).

To help explain the effects of the replacement of Asp167 to Glu, a structure prediction of oxidized PQQGDH-B–glucose complex was carried out using the molecular simulation software Molecular Operating Environment (MOE) (Chemical Computing Group, Quebec, Canada). Based on the predicted structure, we performed molecular dynamics (MD) calculations from 0 to 1 ns with CHARMM22 as a force field and extracted the candidates every 100 fs. Among the extracted structures (10,000 candidates), we determined the structure having the lowest potential energy as a final structure (described in detail in [43]). In our constructed oxidized PQQGDH-B–glucose complex model (Fig. 1A), Asp167 (wild-type) forms a hydrogen bond with the second

Table 2
Kinetic Parameters of PQQGDH-B Wild-type and Asn452Thr

	Wild-type			Asn452Thr		
	K_m (mM)	k_{cat} (s^{-1})	k_{cat}/K_m (s^{-1} mM^{-1})	K_m (mM)	k_{cat} (s^{-1})	k_{cat}/K_m (s^{-1} mM^{-1})
Glucose	25.0	3860	154(100%)	12.5	1791	143(100%)
Allose	35.5	2509	71(46%)	38.7	949	25(17%)
3-*O*-methyl-glucose	28.7	3011	105(68%)	27.6	1253	45(31%)
Galactose	5.3	232	44(29%)	3.7	72	23(16%)
Lactose	18.9	1659	88(57%)	33.6	1038	31(22%)
Maltose	26.0	1930	74(48%)	46.5	1002	15(11%)
Cellobiose	14.0	1355	97(63%)	14.0	1060	76(53%)
Maltotriose	13.9	1230	88(69%)	12.6	457	36(25%)

Table 3
Kinetic Parameters of PQQGDH-Bs for various substrates

	Wild-type			Asp167Glu			Asp167Glu/Asn452Thr		
	K_m (mM)	k_{cat} (s^{-1})	k_{cat}/K_m (s^{-1} mM^{-1})	K_m (mM)	k_{cat} (s^{-1})	k_{cat}/K_m (s^{-1} mM^{-1})	K_m (mM)	k_{cat} (s^{-1})	k_{cat}/K_m (s^{-1} mM^{-1})
Glucose	25.0	3860	154(100%)	55.0	1724	31(100%)	48.0	1193	25(100%)
Allose	35.0	2509	71(45%)	199.0	558	3(10%)	182.0	73	0.4(2%)
3-*O*-methyl-glucose	28.7	3011	105(68%)	99.0	541	6(19%)	198.0	215	1.1(4%)
Galactose	5.3	232	44(29%)	—	—	—	145.0	89	0.6(2%)
Lactose	18.9	1659	88(57%)	77.0	478	6(19%)	55.0	167	3(12%)
Maltose	26.0	1930	74(48%)	156.0	436	3(10%)	147.0	65	0.4(2%)
Cellobiose	14.0	1355	97(63%)	17.0	1073	63(203%)	16.0	226	14(56%)

—, Not determined.

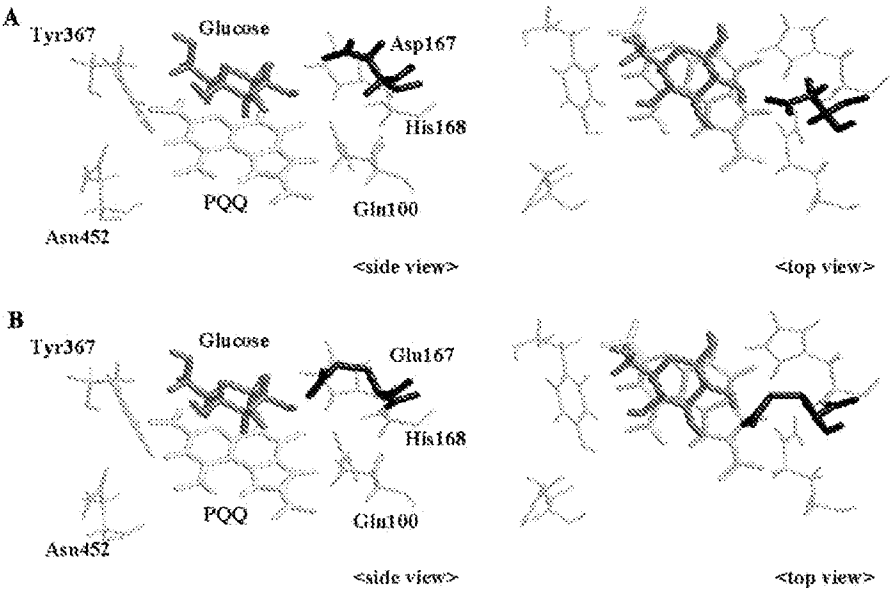

Fig. 1. Predicted structure of the active sites of wild-type (A) and Asp167Glu (B) PQQGDH-Bs.

hydroxyl group of glucose (2.86 Å). On the other hand, in Asp167Glu–glucose complex model (Fig. 1B), Glu167 forms hydrogen bonds with the second (2.22 Å) and third (3.02 Å) hydroxyl groups of glucose without changing the environment of active site. Due to the formation of a new hydrogen bond between Glu167 and the third hydroxyl group, Asp167Glu demonstrated lower reactivity toward allose and 3-*O*-methyl-glucose. Asp167Glu also consistently showed greatly reduced activities with lactose and maltose (Table 3).

The Asp167Glu and Asn452Thr mutations were then combined [41] to investigate the cumulative effect of the two mutations, which individually confer improved specificities. Comparison of the enzymes' substrate specificities showed that Asp167Glu/Asn452Thr has a narrower specificity than both single mutations. The k_{cat}/K_m values of Asp167Glu/Asn452Thr for lactose and maltose are 12 and 2%, respectively, of the value for glucose (Table 3). The catalytic activity of the double mutant (1193 s^{-1}) was comparable to that of the other PQQGDH-Bs, with a K_m value for glucose of 48 mM. The cumulative effect of combining the Asp167Glu and Asn452Thr mutations resulted in a PQQGDH-B with greatly narrowed substrate specificity, while retaining a large proportion of its original catalytic activity.

Thermal stability

The stability of PQQGDH-B is another feature that must be improved for its application as a glucose sensor constituent. The resulting higher yield in active enzyme preparation would improve the cost-effectiveness of glucose sensor production using this enzyme. Furthermore, the recent trend of continuous blood glucose monitoring requires a glucose enzyme sensor capable of continuous operation for several days. Because such sensor chips or electrodes are fabricated with the holo-form of PQQGDH-B for the users' convenience, we focused on evaluating the stability of holo-PQQGDH-B.

Ser231Lys showed the highest thermal stability at 55 °C without decreasing catalytic activity. The half-life

of thermal inactivation at 55 °C was 8-fold greater for Ser231Lys (40 min) than for wild-type (5 min) [39] (Fig. 2A, filled-squares) among Ser231 variants. Using the 3-D structure of PQQGDH-B, we performed a modeling analysis of Ser231Lys indicating that the replacement of Ser231 with Lys significantly increased the hydrophobicity of loop 3CD. This observation suggested that the increase in hydrophobic interaction strengthened the packing of the W motif and/or β-propeller structure. Furthermore, considering the location of Ser231 at the bottom of the β-propeller structure, replacement of this residue was not expected to significantly affect the catalytic properties of this enzyme.

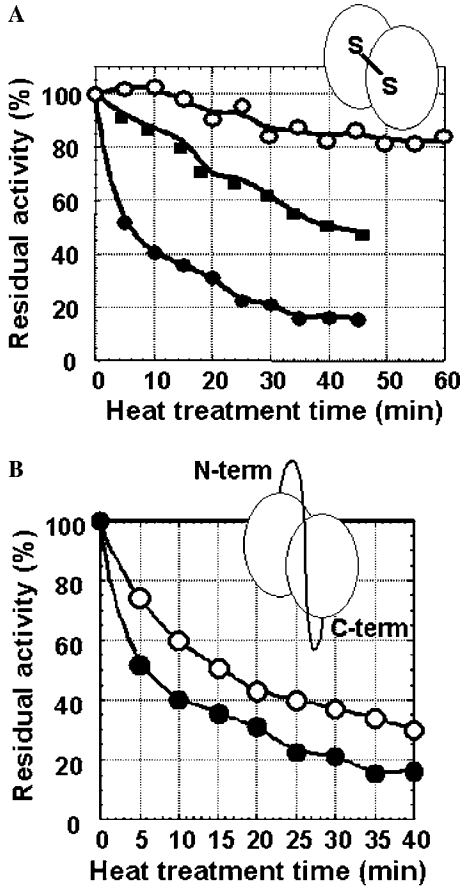

Fig. 2. Thermal stability of engineered PQQGDH-Bs (A) Thermal stability of engineered PQQGDH-B Ser231Lys (■) and Ser415Cys (○) at 55 °C: ○, Ser415Cys; ■, Ser231Lys; and ●, wild-type. (B) Thermal stability of tethered PQQGDH-B at 55 °C: ○, tethered PQQGDH-B; and ●, wild-type.

Assuming that the first step of heat inactivation of PQQGDH-B is dimer dissociation, the stabilization of quaternary structure would be expected to increase the enzyme's thermal stability. Therefore, to decrease the chance of dissociation of PQQGDH-B subunits, we attempted to create (1) chemically cross-linked PQQGDH-B using glutaraldehyde [34], (2) genetically fused PQQGDH-B by the in-frame gene fusion technique [40], and (3) Ser415Cys, which forms a disulfide bond at its dimer interface [42]. Here, we present our efforts in stabilizing PQQGDH-B quaternary structures by protein engineering (Table 4).

Chemically linked PQQGDH-B (mixture of cross-linking status) showed higher thermal stability than wild-type enzyme; the half-life at 55 °C is 63 min whereas that of native enzyme is 5 min [34]. A tethered PQQGDH-B was constructed using the linker peptide Glu-Leu-Gly-Thr-Arg-Gly-Ser-Ser-Arg-Val-Asp-Leu-Gln, derived from the β-galactosidase gene in the pTrc99A expression vector. This enzyme shows enhanced thermal stability (17-min half-life at 55 °C) over the wild-type enzyme (5 min) expressed in *E. coli* (Fig. 2B) [40]. The V_{max} value of tethered PQQGDH-B is 897 U/mg protein with 10–40% of the catalytic activity of the native enzyme. The presence of the linker region prevents complete dissociation of the subunits, thus decreasing the entropy of denaturation with a concomitant increase in the thermal stability. However, the length and flexibility of the linker peptide should be further optimized to construct a thermostable tethered enzyme with appropriate catalytic activity.

Although the stabilization of quaternary structure of PQQGDH-B by chemical modification [34] or tethering with linker peptide [40] improves the thermal stability of PQQGDH-B, these modifications resulted in a decrease in catalytic activity. We therefore attempted to introduce a disulfide bond at the dimer interface of PQQGDH-B to covalently link the two subunits and stabilize the quaternary structure [42]. Searching for residues at the interface that are not associated with the active site but face each other, we identified Ser415, which is located in loop5CD. The distance between each

Table 4
Comparison of the enzymatic properties of engineered PQQGDH-Bs

	Half-life time at 55 °C (min)	Specific activity ($U mg^{-1}$)	K_m (mM)	Catalytic efficiency ($U mg^{-1} mM^{-1}$)	References
Wild-type	5	4610	25	184	[39]
Ser231Lys	40	3313	27	123	[39]
Cross-linking	63[a]	389	20	19.5	[34]
Tethered	16	897	20	45	[40]
Ser415Cys	183	4134	16	258	[42]

[a] Mixture of cross-linking status.

Ser415 side chain is 6.12 Å (Oγ–Oγ), indicating that a disulfide bond may be formed after substitution to a Cys residue. Ser415Cys shows 36-times higher thermal stability at 55 °C than wild-type (half-life: 183 min vs. 5 min) without any decrease in catalytic activity (k_{cat} 3461 s^{-1}) (Fig. 2A, open circles) [42]. Moreover, Ser415Cys retains over 90% of GDH activity after incubation at 70 °C for 10 min. Disulfide bond formation between the subunits was confirmed by SDS–PAGE in the presence and absence of reducing agents. By linking the two subunits with a disulfide bond, the thermal stability of PQQGDH-B was greatly improved. Ser415Cys shows about 4-times higher thermal stability than Ser231Lys at 55 °C (Fig. 2A).

Such a high thermal stability, such as that achieved with Ser415Cys, may enable us to easily prepare enzyme and sensors with little loss of enzyme activity. Our achievement may also extend the use of PQQGDH-B to continuous glucose monitoring (CGM) systems, currently the focus of great attention. The thermal stability of Ser415Cys is higher than that of GOD, thus eliminating an important barrier to its use in CGM systems. Ser415Cys can therefore be used in CGM systems, potentially leading to the development of a more accurate and durable sensor system.

Heterodimeric PQQGDH-B

PQQGDH-B is a homodimeric enzyme composed of 50-kDa subunits with W6-bladed β-propeller structures [24]. Although an active site is located in the center of each propeller structure, the dimeric status is essential for GDH activity. Considering the quaternary structure of PQQGDH-B, the mutations had been introduced at identical positions in each subunit. Therefore, the observed altered enzymatic properties from single amino acid substitutions were the result of the sum of two mutations per homodimeric enzyme. We therefore, developed a novel strategy for the construction of "heterodimeric" PQQGDH-B, of which each subunit harbors a different mutation, as depicted in Fig. 3.

We previously reported Arg-tailed PQQGDH-B showing a different behavior during chromatography as a result of the additional positive charge [46]. Combining this technique with the dissociation/re-dimerization procedure, we developed a method for construction of

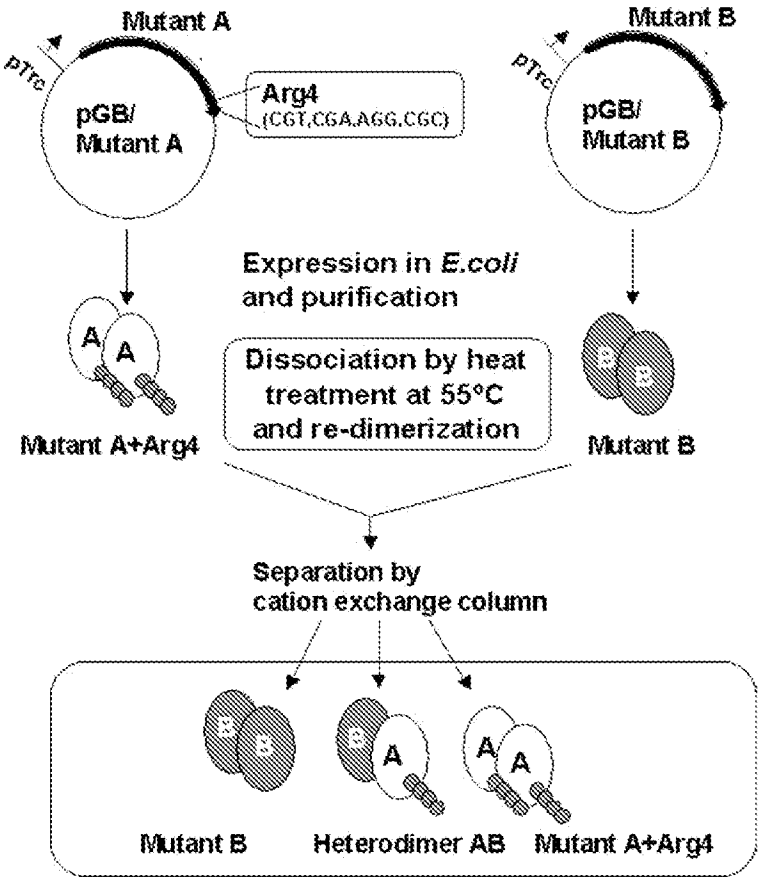

Fig. 3. Preparation of heterodimeric PQQGDH-B from parental homodimeric PQQGDH-B mutants.

heterodimeric soluble PQQGDH-B. By adding an Arg-tail at the C-terminus and mixing with unmodified PQQGDH-B, a heterodimeric enzyme harboring only one Arg-tail is created following the dissociation/re-dimerization procedure. This heterodimeric enzyme can be separated by cation exchange chromatography from homodimers composed of two Arg-tailed subunits and non-tailed subunits.

We first attempted to construct a heterodimeric PQQGDH-B composed of native and inactive mutant subunits. This was achieved by combining Arg-tailed wild-type PQQGDH-B ($4000\,s^{-1}$) with the His168Gln mutant, which showed drastically decreased catalytic activity ($0.8\,s^{-1}$) [43]. Three peaks showing GDH activity were obtained from cation exchange chromatography of the re-dimerized mixture. The middle peak was determined to be heterodimeric wild-type-His168Gln based on several control experiments. The heterodimeric wild-type-His168Gln showed only slightly decreased GDH activity (per wild-type subunit) and similar substrate specificity profile to wild-type an equimolar mixture of wild-type and His168Gln. However, a Hill coefficient of 1.13 for the heterodimeric wild-type-His168Gln indicates positive cooperativity.

We are currently constructing several heterodimers with mutant PQQGDH-Bs showing improved substrate specificity compared with wild-type. These quite unique properties of the resulting heterodimers may lead to further understanding of the mechanism of this enzyme.

Region responsible for enzyme function

In this section, we summarized the region responsible for the functions by the combination of our results with structural information (Table 5 and Fig. 4).

According to 3-D structures, the first hydroxyl group on glucose is recognized by His168, Gln192, and Arg252 [26]. Mutations at His168 showed drastic decreases in catalytic activity and catalytic efficiency [43]. Similarly, Gln192 and Arg252 variants also demonstrated decreased catalytic activity and decreased affinity to substrate. Therefore, recognition of the first hydroxyl group of glucose by the three residues (His168, Gln192, and Arg252) is essential for its high catalytic activity and catalytic efficiency.

Gln100 and Asp167 are located in proximity to the second hydroxyl group of glucose. Most of the 13 Asp167 mutants we constructed and characterized showed similar reactivity towards 2-deoxy-glucose and mannose [43]. In contrast, all our Gln100 variants showed increased reactivity to mannose. These results indicate that the second hydroxyl group is recognized by Gln100. This also suggests that Gln100 can distinguish between glucose and mannose.

The broad substrate specificity profile of PQQGDH-B reflects the absence of residues recognizing the third, fourth, and sixth hydroxyl groups of glucose. According to the enzyme–substrate complex structure, Tyr367 is the nearest residue to the fourth hydroxyl group [26].

Table 5
Impact of mutagenesis

Region	Residues	Interaction with	Imapact of mutagenesis	Corresponding region
Loop1D2A	Gln100	Glc O2	Increase in reactivity for mannose, 3-*O*-methyl-glucose and cellobiose	Region 1
Loop2D3A	Asp167	Glc O2	Decrease in reactivity to allose, 3-*O*-methyl-glucose, lactose and maltose	Region 2
	His168	Glc O1	Drastic decrease in catalytic efficiency	Region 2
Loop3BC	Gln192	Glc O1	Improved substrate specificity but decrease in catalytic activity	Region 2
Loop3D4A	Arg252	Glc O1	Decrease in catalytic activity	Region 3
Loop4BC–4C strand	Asp275	Ca^{2+} (III)	Decreased EDTA tolerance	Region 3
	Asp276	Ca^{2+} (I)	Decreased EDTA tolerance	Region 3
	Glu277	Ca^{2+} (II)	Improved catalytic efficiency	Region 3
	Ile278	None (?)	Decreased K_m value for glucose and enhanced thermal stability	Region 3
	Asn279	Ca^{2+} (III)	Decreased thermal stability	Region 3
Loop4D5A	Tyr367	Glc O4, Lys401, Asn452	No change in substrate specificity profile	
Loop5BC	Lys401	Tyr367	Variable K_m value (19–232 mM) and broader substrate specificity	Region 4
Loop6BC	Asn452	Tyr367	Lower reactivity for lactose and maltose without decrease in catalytic efficiency	Region 4

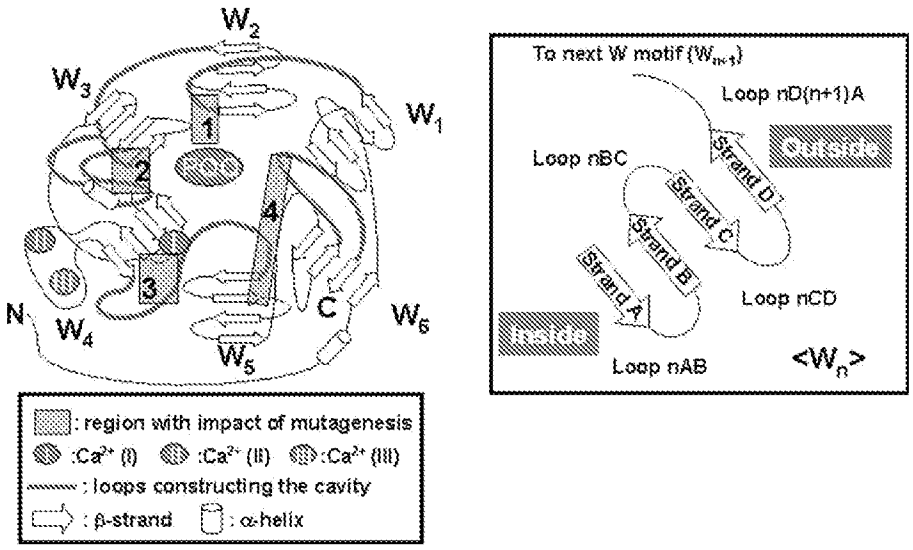

Fig. 4. Secondary structure of topology of PQQGDH-B and regions with impact of mutagenesis.

However, our attempts to substitute Tyr367 failed to alter substrate specificity. According to the 3-D structure, Tyr367 interacts with Lys401 and Asn452 on loop6BC. Asn452 variants showed improved substrate specificity, especially a lower reactivity towards lactose and maltose. We predicted the lack of hydrogen bond between Tyr367 and Asn452 by any substitutions [41]. Therefore, the side chain position of Tyr367 facing the fourth hydroxyl group of glucose may cause steric hindrance preventing lactose to enter the cavity. In contrast, Lys401 mutants showed broader substrate specificity compared with wild-type (unpublished data), with K_m values varying considerably (from 19 to 232 mM). Although substitution of Tyr367 did not affect the substrate specificity profile, substitutions of Lys401 and Asn452 have the significantly effects. These implied that the analysis of the network near Tyr367 might be important.

As already described, mutation of the Ca^{2+}-binding residues Glu277, Asp275, Asp276, and Asn279 affects catalytic activity, substrate specificity, thermal stability, and EDTA tolerance [25]. Because these residues are located near the active site and dimer interface, they are related to both the active-site formation of dimerization.

Our results described in this review may serve as a guide in further engineering of PQQGDH-B. Moreover, they will give effective information about unknown properties on PQQGDH-B such as reaction mechanism, substrate inhibition, and negative cooperativity.

Application of engineered PQQGDHs

The molecular engineering of PQQGDH is aimed at the development of an ideal enzyme for glucose sensing. The construction of stable PQQGDH enabled us to expand the application of PQQGDH not only for the disposable (finger-stick) type sensors, but also for flow injection analysis (FIA) systems as well as the newly important continuous glucose monitoring systems. In addition to the improvement of stability and substrate specificity of PQQGDH, further improvements of electron transfer with electron mediators and electrodes are also expected. Considering the high catalytic efficiency of PQQGDH and the simple methods and devices to electrochemically detect its activity encouraged us to investigate other useful applications of this enzyme. In this section, we summarize the possible applications of engineered glucose dehydrogenases for glucose sensing, biofuel cell systems, as well as an enzyme probe for electrochemical DNA sensors.

Glucose sensors based on engineered PQQGDH-Bs

As Ser231Lys showed significantly increased thermal stability while retaining almost identical catalytic activity as the wild-type enzyme, we applied the mutant to the construction of a glucose enzyme sensor with increased operational stability. The resulting glucose sensor showed extremely high stability, retaining over 80% of its initial activity after incubation at 60 °C for 2 h [34]. In contrast, an electrode constructed with native PQQGDH-B retained only 30% of its initial activity.

Chemical modification has been widely utilized to increase enzyme stability, although cross-linking often results in a decrease in catalytic efficiency. However, since PQQGDH-B loses its activity upon dissociation of its quaternary structure (Fig. 2), chemical cross-linking modification was expected to help stabilize the enzyme. We constructed an FIA system for glucose measurement by immobilizing glutaraldehyde cross-linked PQQGDH-B

onto an electrode. The cross-linked PQQGDH-B had high thermal stability, with a half-life at 55 °C of 63 min, whereas that of the native enzyme was 5 min. The resulting FIA system employing cross-linked PQQGDH-B showed high operational stability with very stable response to glucose injection [34].

For each sensor system, the sensor signal is also greatly dependent on the type of mediator employed due to the preference of this enzyme toward artificial electron mediators [30,47,48]. For example, PQQGDH shows high catalytic current when phenazine methosulfate (PMS) or ruthenium complex was utilized as the mediator. However, PQQGDH does not efficiently utilize potassium ferricyanide, a stable and cost effective mediator used in a large number of electrochemical sensors. The further improvement of mediator preference of PQQGDH is therefore required. To improve mediator-dependent sensor signal, we focused on the application of electron transfer proteins, cytochromes, as interface molecules to facilitate the electron transfer from enzyme to artificial electron mediator. We used cytochrome *c* and cytochrome b_{562} for the sensor signal improvement of glucose enzyme sensors employing PQQGDH. When sensors were operated using either potassium ferricyanide or 1-methoxy-5-methylphenazinium methylsulfate (mPMS) as the artificial electron mediator, the response was over 30-fold greater with the co-immobilization of either cytochrome *c* (cyt *c*) or cytochrome b_{562} (cyt b_{562}) than with PQQGDH-B alone [35]. The impact of the cytochrome co-immobilization was dependent on the amount of cytochrome, indicating that these cytochromes facilitated the electron transfer from the PQQGDH redox center to the artificial electron mediators used in the sensor systems. These results suggest the future application of cytochromes as an essential component for the improvement of sensor response in the redox enzyme-based amperometric sensors.

Considering the recent trend in the development of implantable enzyme sensors, such as for continuous glucose monitoring, mediatorless or direct electron transfer enzyme sensors are preferable to the utilization of low molecular weight artificial electron mediators. Continuous glucose monitoring is expected to become an ideal way to monitor glycemic levels in diabetic patients. However, due to a number of limitations of PQQGDH, the conventionally utilized GOD remains the preferred enzyme for CGM. Two major problems that arose in the application of PQQGDH for CGM are the poor stability and its requirement for artificial electron acceptors for electrochemical measurement. In most oxidoreductases, including PQQGDH, the prosthetic group is buried deeply within the protein shell. Direct electrochemical recycling of the enzyme's prosthetic group at the electrode surface, leading to a corresponding current signal, is therefore rarely encountered. One possible solution to these problems is to use redox polymers such as Os complex-modified polypyrrole polymer, as demonstrated with a reagentless glucose sensor employing PQQGDH-A from *Erwinia* sp. 34-1 [49].

Because toxic chemicals such as Os should be avoided in implantable enzyme sensors, we applied an engineered PQQGDH-B with cyt b_{562} as electron acceptor. We constructed a PQQGDH-B electrode co-immobilized with cyt b_{562} and investigated the electrochemical properties without synthetic electron mediators. PQQGDH-B/cyt b_{562} electrode responded well to glucose, whereas no current increase was observed from the electrode immobilizing enzyme alone [36]. The engineered PQQGDH-B Ser415Cys, which has a far superior thermal stability over the wild-type enzyme (Fig. 2A) [42], was applied for the construction of CGM system. As a result, the operational stability of CGM system employing Ser415Cys co-immobilized with cyt b_{562} was far superior to that of the wild-type enzyme-based electrode, with more than 60% of the initial response observed after 72 h at 37 °C [38]. We have achieved the construction of a synthetic mediator-free PQQGDH-based CGM system.

We extended the above idea by genetically fusing PQQGDH-B to cytochrome to enable electron transfer to the electrode in the absence of artificial electron mediator. The fusion protein mimics the domain structure of the quinohemoprotein ethanol dehydrogenase (QH-EDH) from *Comamonas testosteroni*, which contains an additional heme *c* prosthetic group together with PQQ (Fig. 5). The fusion of the cytochrome *c* domain of QH-EDH to the C-terminus of PQQGDH-B showed not only intra-molecular electron transfer, between PQQ and heme of the cytochrome *c* domain, but also electron transfer from heme to the electrode [37]. The fusion protein thus allows the construction of a direct electron transfer-type glucose sensor, enabling us to construct a continuous glucose monitoring system using engineered QH-GDH.

Other applications of engineered PQQGDH-B; biofuel cells and DNA sensors

Biofuel cell systems utilize biocatalysts, such as enzymes and microorganisms, as the anodic electrocatalysts, instead of transition metal catalysts utilized in conventional fuel cell systems. Several organic compounds can be utilized in biofuel cells, such as biomass sugars and alcohols. A more efficient energy conversion can theoretically be achieved with biofuel cells than with transition metal-based fuel cells. A recent trend in the development of biofuel cell has been in the use of glucose as the fuel to be oxidized by GOD at the bioanode, combined with an appropriate biocathode employing several dioxygen reducing enzymes [50–54]. PQQGDH's insensitivity to oxygen makes it a favorable enzyme for

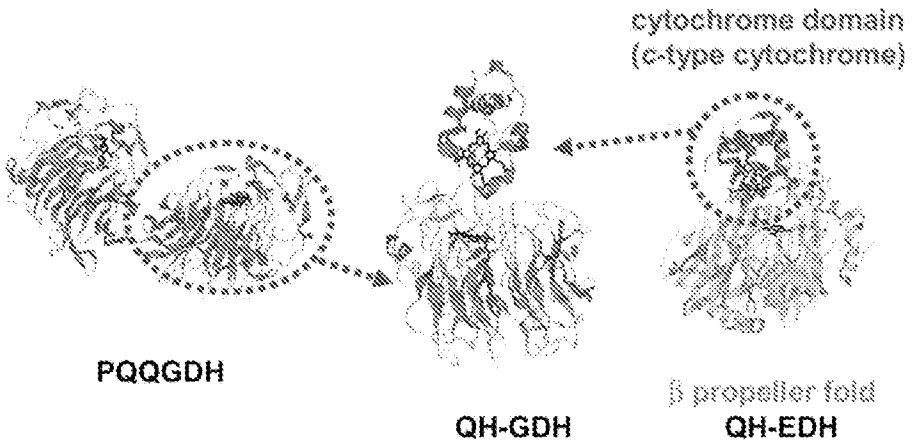

Fig. 5. Construction of QH-GDH.

the bioanode. Ikeda and co-workers [55,56] reported biofuel cells employing PQQGDH and NAD-dependent GDH instead of GOD. However, the application of PQQGDH for the bioanode is inherently limited because of its instability. We, therefore, constructed a glucose biofuel cell system employing at the anode the Ser415Cys mutant of PQQGDH-B, whose stability was greatly improved by protein engineering [42], and bilirubin oxidase (BOD) at the cathode. The lifetime of the resulting biofuel cell system employing engineered Ser415Cys PQQGDH-B was greatly extended compared with that employing wild-type PQQGDH-B [38].

DNA sensing has become a very powerful tool for diagnosis, detection of the toxic microorganisms in food or the environment, and in fundamental molecular biology research. An electrochemical DNA sensing system would be a very promising tool since it only requires an electrode and an electrochemical analysis system, resulting in a simple detection system. Many types of electrochemical DNA sensors using DNA-immobilized electrodes have been developed [57–59], most of which are based on the detection of hybridization. Some reported examples include the use of redox intercalators to recognize double stranded DNA [60,61], DNA detection via a DNA-mediated electron transfer to the electrode using mediators [62–64], and the use of ferrocene-labeled oligonucleotide probes that hybridize to DNA immobilized on the electrode [65]. To improve the sensitivity, enzyme labels have been used for the detection of hybridization since they can dramatically amplify the signal. PQQGDH-B seemed to be a promising candidate as a labeling enzyme since it uses glucose as a substrate. The O_2 insensitivity and high catalytic activity of PQQGDH-B make it a very suitable label [66]. Moreover, PQQGDH-B activity can be measured amperometrically, which is the most frequently used method in routine electrochemical detection systems because of its simplicity. An amperometric DNA sensor using PQQGDH-B may therefore be an ideal electrochemical DNA detection system. However, the high operational temperature usually employed for the selective annealing process would inactivate the enzyme probe. We therefore, investigated the possibility of using our engineered PQQGDH-B as a probe enzyme in DNA sensing.

We first constructed a novel amperometric DNA sensor employing wild-type PQQGDH-B conjugated with avidin for labeling of the hybridization product. Since DNA can be easily labeled with biotin, we chose to detect DNA hybridization via biotin–avidin binding. An oligonucleotide was then immobilized on a carbon paste electrode and its hybridization with the biotinylated target oligonucleotide was detected. The electric current is generated from glucose oxidization catalyzed by PQQGDH-B via m-PMS electron mediator (Fig. 6A). The sensor response increased with the addition of glucose and the response increased with increasing DNA [67]. Since our sensor showed a highly sensitive and selective response to the target DNA, a broad range of applications to many types of samples are expected. For rapid and simple DNA detection, a thermostable engineered PQQGDH-B was preferred. The engineered Ser415Cys PQQGDH-B [42] enables the operation of PQQGDH-B based DNA sensors at the higher hybridization temperatures, consequently reducing the operational steps and increasing the accuracy of DNA detection. We prepared Ser415Cys PQQGDH-B–avidin conjugate by using glutaraldehyde to label probe DNA via biotin (Fig. 6B). To fabricate the sensor, an oligonucleotide was immobilized on an Au electrode and its hybridization with the probe DNA was detected by measuring the electric current generated by Ser415Cys PQQGDH-B with the addition of glucose. The sensor response dependence on glucose and DNA concentrations was investigated and the detection of asymmetric PCR product was also performed. Ser415Cys PQQGDH-B-labeled probe DNA was hybridized with the immobilized DNA at 60 °C for 10 min and then the

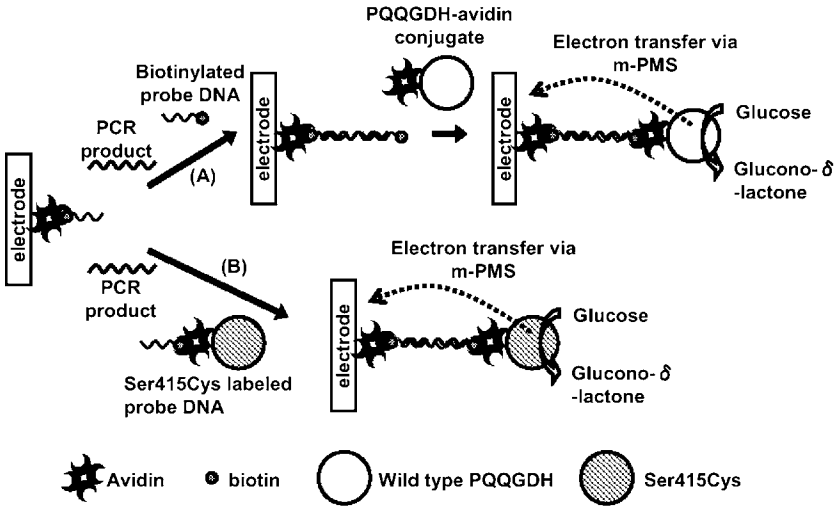

Fig. 6. DNA sensor using PQQGDH-B for signal amplification. (A) DNA sensor using wild-type PQQGDH-B. (B) DNA sensor using Ser415Cys.

resulting electric current generated from Ser415Cys PQQGDH-B by glucose addition was measured [68]. This sensor was able to distinguish 4.0 nM target DNA from control DNA and showed good selectivity, distinguishing a 3-base difference. It can also selectively detect approximately 4 nM of asymmetric PCR product by the sandwich method. This sensor system can be applied to the detection of single nucleotide polymorphisms (SNP) in the same manner as reported by Patolsky et al. [69]. It therefore has a broad range of potential applications with various types of samples.

Summary

PQQGDHs are the most industrially attractive enzymes especially PQQGDH-B employing glucose sensors are already in the market. To develop an ideal glucose sensor enzyme, therefore we have constructed and characterized several engineered PQQGDH-Bs. Our recent advances in protein engineering indicate that Glu277Lys, Asn452Thr, Asp167Glu, Asp167Glu/Asn452Thr, and Ser415Cys may be the most versatile and ideal for glucose sensors. Moreover, our recent results will be the guide in engineering of PQQGDH-B. They will give effective information about unknown properties on PQQGDH-B such as reaction mechanism, substrate inhibition system, and negative cooperativity.

Of equal importance, the application of the thermostable PQQGDH-B is not limited to the development of continuous glucose monitoring system, biofuel cell, and DNA sensors. In addition, co-immobilizing electron transfer protein such as cytochrome *c* and cytochrome b_{562}, we have developed the sensor system that showed 30-fold greater response. Furthermore, mimicking the domain structure of QH-EDH, we constructed fusion protein, QH-GDH, allowing the construction of a direct electron transfer-type glucose sensor. To the future, combining the engineered PQQGDH-B with the application of cytochromes instead of artificial electron mediator, we will construct and develop the ideal glucose sensor and other applications.

Acknowledgment

The authors thank Dr. Stefano Ferri for kindly revising the manuscript.

References

[1] K. Matsushita, E. Shinagawa, O. Adachi, M. Ameyama, Biochemistry 28 (1989) 6276–6280.
[2] A.M. Cleton-Jansen, N. Goosen, T.J. Wenzel, P. van de Putte, J. Bacteriol. 170 (1988) 2121–2125.
[3] K. Matsushita, O. Adachi, in: V. Davidson (Ed.), Principles and Applications of Quinoproteins, Dekker, New York, 1993, pp. 245–273.
[4] A.M. Cleton-Jansen, N. Goosen, G. Odle, P. van de Putte, Nucleic Acids Res. 16 (1988) 6228.
[5] A.M. Cleton-Jansen, N. Goosen, O. Fayet, P. van de Putte, J. Bacteriol. 172 (1990) 6308–6315.
[6] K. Matsushita, Y. Ohno, E. Shinagawa, O. Adachi, M. Ameyama, Agric. Biol. Chem. 46 (1982) 1007–1011.
[7] M. Beardmore-Gray, C. Anthony, J. Gen. Microbiol. 132 (1986) 1257–1268.
[8] G.E. Cozier, C. Anthony, Biochem. J. 312 (1995) 679–685.
[9] A.B. Witarto, S. Ohuchi, M. Narita, K. Sode, J. Biochem. Mol. Biol. Biophys. 2 (1999) 209–213.
[10] M. Yamada, K. Sumi, K. Matsushita, O. Adachi, Y. Yamada, J. Biol. Chem. 268 (1993) 12812–12817.
[11] K. Sode, H. Sano, Biotechnol. Lett. 16 (1994) 455–460.
[12] K. Sode, K. Watanabe, S. Ito, K. Matsumura, T. Kikuchi, FEBS Lett. 364 (1995) 325–327.
[13] K. Sode, H. Yoshida, K. Matsumura, T. Kikuchi, M. Watanabe, N. Yasutake, S. Ito, H. Sano, Biochem. Biophys. Res. Commun. 211 (1995) 268–273.

[14] K. Sode, K. Kojima, Biotechnol. Lett. 19 (1997) 1073–1077.
[15] K. Sode, H. Yoshida, Denki Kagaku 65 (1997) 444–451.
[16] H. Yoshida, K. Sode, J. Biochem. Mol. Biol. Biophys. 1 (1997) 89–93.
[17] J. Okuda, H. Yoshida, K. Kojima, M. Himi, K. Sode, J. Biochem. Mol. Biol. Biophys. 4 (2000) 415–422.
[18] H. Yoshida, K. Kojima, A.B. Witarto, K. Sode, Protein Eng. 12 (1999) 63–70.
[19] L.D. Elias, M. Tanaka, H. Izu, K. Matsushita, O. Adachi, M. Yamada, J. Biol. Chem. 275 (2000) 7321–7326.
[20] L.D. Elias, M. Tanaka, M. Sakai, M. Toyama, K. Matsushita, O. Adachi, M. Yamada, J. Biol. Chem. 276 (2001) 48356–48361.
[21] G.E. Cozier, R.A. Salleh, C. Anthony, Biochem. J. 340 (1999) 639–647.
[22] A.M. Cleton-Jansen, N. Goosen, K. Vink, P. van de Putte, Mol. Gen. Genet. 217 (1989) 430–436.
[23] P. Dokter, J. Frank, J.A. Duine, Biochem. J. 239: (1986) 163–167.
[24] A. Oubrie, H.J. Rozeboom, K.H. Kalk, J.A. Duine, B.W. Dijkstra, J. Mol. Biol. 289 (1999) 319–333.
[25] S. Igarashi, T. Ohtera, H. Yoshida, A.B. Witarto, K. Sode, Biochem. Biophys. Res. Commun. 264 (1999) 820–824.
[26] A. Oubrie, H.J. Rozeboom, K.H. Kalk, A.J.J. Olsthoorn, J.A. Duine, B.W. Dijkstra, EMBO J. 18 (1999) 5187–5194.
[27] A.E.G. Cass, D.G. Francis, H.A.O. Hill, W.J. Aston, I.J. Higgins, E.V. Plotkin, L.D. Scott, A.P.F. Turner, Anal. Chem. 56 (1984) 667–671.
[28] D.R. Matthews, R.R. Holman, E. Brown, J. Steemson, A. Watson, S. Hughes, D. Scott, Lancet 4 (1987) 778–779.
[29] Y. Degani, A. Heller, J. Phys. Chem. 91 (1987) 1285–1288.
[30] E.J. D'Costa, I.J. Higgins, A.P.F. Turner, Biosensors 2 (1986) 71–87.
[31] L. Ye, M. Hammerle, A.J.J. Olsthoorn, W. Schuhmann, H.L. Schmidt, J.A. Duine, A. Heller, Anal. Chem. 65 (1993) 238–241.
[32] G.J. Kost, H.T. Vu, J.H. Lee, P. Bourgeois, F.L. Kiechle, C. Martin, S.S. Miller, A.O. Okorodudu, J.J. Podczasy, R. Webster, K.J. Whitlow, Crit. Care Med. 26 (1998) 581–590.
[33] H. Yoshida, T. Iguchi, K. Sode, Biotechnol. Lett. 22 (2000) 1505–1510.
[34] Y. Takahashi, S. Igarashi, Y. Nakazawa, W. Tsugawa, K. Sode, Electrochemistry 68 (2000) 907–911.
[35] J. Okuda, J. Wakai, K. Sode, Anal. Lett. 35 (2002) 1465–1478.
[36] J. Okuda, J. Wakai, N. Yuhashi, K. Sode, Biosens. Bioelectron. 18 (2003) 699–704.
[37] J. Okuda, K. Sode, Biochem. Biophys. Res. Commun. 314 (2004) 793–797.
[38] J. Okuda, J. Wakai, S. Igarashi, K. Sode, Anal. Lett. 37 (2004) 1871–1881.
[39] K. Sode, T. Ohtera, M. Shirahane, A.B. Witarto, S. Igarashi, H. Yoshida, Enzyme Microb. Technol. 26: (2000) 491–496.
[40] K. Sode, M. Shirahane, H. Yoshida, Biotechnol. Lett. 21 (1999) 707–710.
[41] K. Sode, S. Igarashi, A. Morimoto, H. Yoshida, Biocatal. Biotransform. 20 (2002) 405–412.
[42] S. Igarashi, K. Sode, Mol. Biotechnol. 24 (2003) 97–103.
[43] S. Igarashi, T. Hirokawa, K. Sode, Biomol. Eng. 21 (2004) 81–89.
[44] K. Kojima, A.B. Witarto, K. Sode, Biotechnol. Lett. 22 (2000) 1343–1347.
[45] H. Yoshida, N. Araki, A. Tomisaka, K. Sode, Enzyme Microb. Technol. 13 (2002) 312–318.
[46] H. Koh, S. Igarashi, K. Sode, Biotechnol. Lett. 25 (2003) 1695–1701.
[47] T.J. Ohara, R. Rajagopalan, A. Heller, Anal. Chem. 66 (1994) 2451–2457.
[48] K. Matsushita, E. Shinagawa, O. Adachi, M. Ameyama, J. Biochem. (Tokyo) 105 (1989) 633–637.
[49] K. Habermuller, A. Ramanavicius, V. Laurinavicius, W. Schuhmann, Electroanalysis 12 (2000) 1383–1389.
[50] E. Katz, I. Willner, A.B. Kotlyar, J. Electroanal. Chem. 479 (1999) 64–68.
[51] H.H. Kim, N. Mano, X.C. Zhang, A. Heller, J. Electrochem. Soc. 150 (2003) A209–A213.
[52] N. Mano, H.H. Kim, A. Heller, J. Phys. Chem. B 106 (2002) 8842–8848.
[53] N. Mano, H.H. Kim, Y.C. Zhang, A. Heller, J. Am. Chem. Soc. 124 (2002) 6480–6486.
[54] T. Chen, S.C. Barton, G. Binyamin, Z.Q. Gao, Y.C. Zhang, H.H. Kim, A. Heller, J. Am. Chem. Soc. 123 (2001) 8630–8631.
[55] S. Tsujimura, K. Kano, T. Ikeda, Electrochemistry 70 (2002) 940–942.
[56] S. Tsujimura, K. Kano, T. Ikeda, Chem. Lett. (10) (2002) 1022–1023.
[57] S. Mikkelsen, Electroanalysis 8 (1996) 15–19.
[58] E. Palecek, Electroanalysis 8 (1996) 7–14.
[59] J. Wang, Chem. Eur. J. 70 (1999) 3699–3702.
[60] K. Hashimoto, K. Ito, Y. Ishimori, Sensor. Actuator. B 46 (1998) 220–225.
[61] G. Marrazza, S. Tombelli, M. Mascini, A. Manzoni, Clin. Chim. Acta. 307 (2001) 241–248.
[62] F. Lisdat, B. Ge, B. Krause, A. Ehrlich, H. Bienert, F.W. Scheller, Electroanalysis 13 (2001) 1225–1230.
[63] G. Hartwich, D.J. Caruana, T. De Lumley-Woodyear, Y. Wu, C.N. Campbell, A. Heller, J. Am. Chem. Soc. 121 (1999) 10803–10812.
[64] E.M. Boon, D.M. Ceres, T.G. Drummond, M.G. Hill, J.K. Barton, Nat. Biotechnol. 18 (2000) 1096–1100.
[65] T. Ihara, Y. Maruo, S. Takenaka, M. Takagi, Nucleic Acids Res. 24 (1996) 4273–4280.
[66] L. Ye, A. Heller, A.M. Hammerle, W. Schuhmann, H.L. Schmidt, A.J.J. Olsthoorn, J.A. Duine, Abstr. Pap. Am. Chem. Soc. 205 (1993) 34-IEC.
[67] K. Ikebukuro, Y. Kohiki, K. Sode, Biosens. Bioelectron. 17 (2002) 1075–1080.
[68] K. Ikebukuro, Y. Saito, S. Igarashi, K. Sode, Electrochemistry 71 (2003) 490–495.
[69] F. Patolsky, A. Lichtenstein, I. Willner, Nat. Biotechnol. 19 (2001) 253–257.